powers were 543 and 0mW, respectively. The TDF lengths were set so that the product of Tm^{3+} concentration and fibre lengths equalled 40000 ppm.m. The Figure shows that the gain peak shifts from 1473 to 1505nm (32nm shift) as the Tm^{3+} concentration increases from 2000 to 8000ppm. The NF remains low for the various Tm^{3+} concentrations. These results confirmed the validity of our proposed high Tm^{3+} concentration doping technique.

Fig. 3 shows the gain spectrum and NF when the TDF length was 13.3m, the Tm^{3+} concentration was 6000ppm, and the forward and backward pump powers were 325 and 175mW, respectively. The TDFA achieved a gain of > 18dB and an NF of < 7dB in the 1480–1510nm wavelength region. The output power was 14.1dBm.

Conclusion: We have realised a novel gain-shifted TDFA by doping TDF with a high thulium concentration. The gain peak shifted from 1473 to 1505nm as the Tm^{3+} concentration increased from 2000 to 8000ppm. In a gain-shifted TDFA with a Tm^{3+} concentration of 6000ppm we have achieved a gain of > 18dB and an NF of < 7dB in the 1480–1510nm wavelength region for a pump power of 500mW.

Acknowledgments: The authors thank K. Kobayashi, K. Shikano, K. Kato, K. Oikawa and T. Miya for useful discussions and support throughout the course of this work.

7 January 2000
Electronics Letters Online No: 20000332
DOI: 10.1049/el:20000332

S. Aozasa, T. Sakamoto, T. Kanamori, K. Hoshino and M. Shimizu (*NTT Photonics Laboratories, Tokai, Naka, Ibaraki, 319-1193, Japan*)

References

1 ELBERS, J.-P., SCHEERER, C., FARBERT, A., GLINGENER, C., SCHOPFLIN, A., GOTTWALD, E., and FISCHER, G.: '3.2Tbit/s (80x40Gbit/s) bi-directional DWDM/ETDM transmission'. ECOC'99, 1999, Paper PD2-5

2 NAITO, T., SHIMOJOH, N., TANAKA, T., NAKAMOTO, H., DOI, M., UEKI, T., and SUYAMA, M.: '1 terabit/s WDM transmission over 10,000 km'. ECOC'99, 1999, Paper PD2-1

3 KANI, J., HATTORI, K., JINNO, M., AIZAWA, S., SAKAMOTO, T., and OGUCHI, K.: 'Trinal-wavelength-band WDM transmission over dispersion-shifted fibre', *Electron. Lett.*, 1999, **35**, (4), pp. 321–322

4 KASAMATSU, T., YANO, Y., and SEKITA, H.: 'Novel 1.50-μm band gain-shifted thulium-doped fibre amplifier by using dual wavelength pumping of 1.05μm and 1.56μm'. OAA'99, 1999, Paper PDP1

5 KOMUKAI, T., YAMAMOTO, T., SUGAWA, T., and MIYAJIMA, Y.: 'Upconversion pumped thulium-doped fluoride fibre amplifier and laser operating at 1.47μm', *IEEE J. Quantum Electron.*, 1995, **QE-31**, (11), pp. 1880–1889

6 PERCIVAL, R.M., and WILLIAMS, J.R.: 'Highly efficient 1.064μm upconversion pumped 1.47μm thulium doped fluoride fibre amplifier', *Electron. Lett.*, 1994, **30**, (20), pp. 1684–1685

Direct algorithm for rectifying pairs of uncalibrated images

K.A. Al-Shalfan, J.G.B. Haigh and S.S. Ipson

Given the fundamental matrix connecting two uncalibrated images of a 3D scene, a convenient procedure is presented for determining transformations to make corresponding points lie on the same horizontal lines. The method is illustrated using two images of a calibration cube, one of many successful applications.

An important stage in the three-dimensional interpretation of two images of a scene, with lateral displacement between the viewpoints, is the production of a pair of rectified images; the depth of a point in the scene may then be related to horizontal disparity. Received methods of rectification either require some knowledge of the camera calibration [1, 2] or involve some decision making to determine the optimal transformation [3, 4]. In this Letter we describe a general and unambiguous method for the rectification of images from an uncalibrated camera, directly from the fundamental equation describing the relationship between them.

Suppose that the homogeneous co-ordinates of a point in image 1 are given by the vector $\mathbf{x}$ and those of the corresponding point in image 2 by $\mathbf{x}'$; then $\mathbf{x}$ and $\mathbf{x}'$ are related by the fundamental equation

$$\mathbf{x}'^T F\mathbf{x} = 0 \tag{1}$$

where the fundamental matrix F is a 3×3 matrix of rank 2. The eight-point algorithm may be used to determine the elements of F from the co-ordinates of at least eight pairs of matching points, but care must be taken to ensure that the calculation is well-conditioned [5]. The matrix F describes the epipolar geometry of the two images; the homogeneous co-ordinates $\mathbf{e} = [e_1\ e_2\ 1]^T$ of the epipole in image 1 and those $\mathbf{e}' = [e'_1\ e'_2\ 1]^T$ of the epipole in image 2 are the right and left eigenvectors of F corresponding to the zero eigenvalue: $F\mathbf{e} = \mathbf{0}$ and $\mathbf{e}'^T F = \mathbf{0}^T$.

The aim of rectification is to apply homographic transformations $\mathbf{X} = A\mathbf{x}$ and $\mathbf{X}' = B\mathbf{x}'$, ensuring that corresponding epipolar lines in the two images are transformed into horizontal lines at the same vertical location. Expressed in terms of the homogeneous co-ordinates, this means that

$$\frac{X_2}{X_3} = \frac{X'_2}{X'_3}$$

$$\therefore \quad X_2X'_3 = X_3X'_2$$

$$\therefore \quad (a_{21}x_1 + a_{22}x_2 + a_{23}x_3)(b_{31}x'_1 + b_{32}x'_2 + b_{33}x'_3) = (a_{31}x_1 + a_{32}x_2 + a_{33}x_3)(b_{21}x'_1 + b_{22}x'_2 + b_{23}x'_3)$$

$$\therefore \quad \mathbf{x}'^T C\mathbf{x} = 0 \tag{2}$$

where

$$C = \begin{bmatrix} a_{21}b_{31} - a_{31}b_{21} & a_{22}b_{31} - a_{32}b_{21} & a_{23}b_{31} - a_{33}b_{21} \\ a_{21}b_{32} - a_{31}b_{22} & a_{22}b_{32} - a_{32}b_{22} & a_{23}b_{32} - a_{33}b_{22} \\ a_{21}b_{33} - a_{31}b_{23} & a_{22}b_{33} - a_{32}b_{23} & a_{23}b_{33} - a_{33}b_{23} \end{bmatrix} \tag{3}$$

Since eqn. 2 is identical in form to the fundamental eqn. 1, which the vectors $\mathbf{x}$ and $\mathbf{x}'$ must satisfy, it is equivalent to eqn. 1. Hence the elements of C are proportional to those of F; this provides a necessary and sufficient condition for the matrices A and B to define appropriate rectifying transformations.

We have derived one solution for A and B from the singular value decomposition of F, but this has not proved to be very satisfactory, since the rectified images are often very distorted. Instead we have adopted a more direct approach which starts by the construction of a transformation to move the epipole $\mathbf{e}$ in image 1 an infinite distance along the x-axis:

$$A = \begin{bmatrix} 1 & 0 & 0 \\ -e_2/e_1 & 1 & 0 \\ -1/e_1 & 0 & 1 \end{bmatrix} \tag{4}$$

so that $\mathbf{E} = A\mathbf{e} = [e_1\ 0\ 0]^T$. If $|e_2| > |e_1|$, it is appropriate to interchange the x and y co-ordinates of the images. If either epipole is within the image then rectification is not appropriate and the algorithm should terminate. Substitution of the elements of A from eqn. 4 into eqn. 3 gives

$$C = \begin{bmatrix} -e_2b_{31}/e_1 + b_{21}/e_1 & b_{31} & -b_{21} \\ -e_2b_{32}/e_1 + b_{22}/e_1 & b_{32} & -b_{22} \\ -e_2b_{33}/e_1 + b_{23}/e_1 & b_{33} & -b_{23} \end{bmatrix}$$

The second and third columns of C may be made proportional to those of F by setting $b_{3i} = f_{i2}$ and $b_{2i} = -f_{i3}$. A typical element in the first column is then $-(e_2f_{i2} + f_{i3})/e_1$, or $-(-e_1f_{i1})/e_1 = f_{i1}$ since $F\mathbf{e} = \mathbf{0}$, and is also proportional to the element of F. Hence the appropriate form for B to match A in eqn. 4 is

$$B = \begin{bmatrix} b_{11} & b_{12} & b_{13} \\ -f_{13} & -f_{23} & -f_{33} \\ f_{12} & f_{22} & f_{32} \end{bmatrix} \tag{5}$$

As the three elements by b_{1j} of the first row of B remain undetermined, they may be used to ensure that three selected pairs of

points have the same locations in both rectified images; this is simply a matter of setting up and solving three simultaneous linear equations. The three points define a reference plane for the disparity map, and a sensible choice will assist a human interpreter during the final stages of reconstruction, without affecting the accuracy of the computer calculations. Alternatively, three widely separated points may be automatically selected.

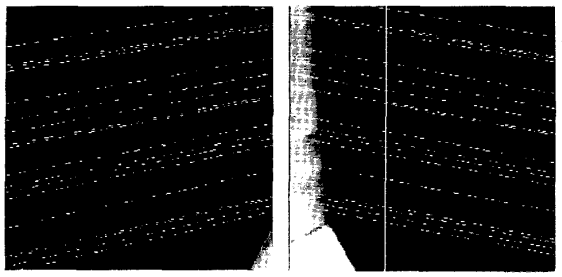

667/1

Fig. 1 *Images of left and right views of cube with epipolar lines superimposed*

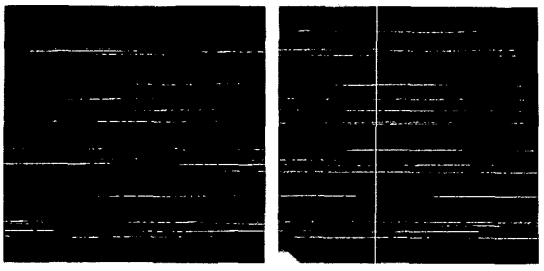

667/2

Fig. 2 *Images of left and right views of cube after rectification*

The method has been applied successfully to a wide variety of images including computer-generated models, laboratory test rigs, architectural images and aerial photographs of rural and urban areas. Images have been captured using a TV camera with a frame-grabber, a high-resolution digital camera and a flatbed scanner. A typical example is shown in Fig. 1, where two 512 by 512 pixel images of a calibration cube of side 30cm have been captured with a Cohu TV camera (model 4712) and a Matrox PIP 1024 frame-grabber. The fundamental matrix was determined using the eight-point algorithm with 18 pairs of manually selected points, at the intersections of orthogonal lines engraved on the faces of the cube. The epipolar lines corresponding to the selected points are superimposed on the images. The calculated root-mean-square perpendicular distance between point and corresponding epipolar line is 0.67 pixels.

The results of the rectification procedure are shown in Fig. 2 where the resampled intensities are taken from the nearest pixel in the original images. It is apparent that all the epipolar lines are horizontal and there is good agreement between the vertical positions of corresponding epipolar lines. The agreement is not perfect, reflecting the error in locating the original pairs of corresponding points. No computational procedure has been applied to reduce the errors since the results indicate typically what is achieved with significant errors of observation. The rectified images are a useful aid for finding further correspondences between the original images images and hence to reconstruction of the 3D scene. We have completed such a 3D reconstruction of points on the cube, but the details are beyond the scope of the current Letter.

The rectification procedure specified by eqns. 4 and 5 is straightforward and has worked reliably in each of the many cases on which it has been tested. The general user is likely to find it more convenient than any other method, to the best of our knowledge.

17 January 2000
Electronics Letters Online No: 20000362
DOI: 10.1049/el:20000362

K.A. Al-Shalfan, J.G.B. Haigh and S.S. Ipson (*Department of Electronic and Electrical Engineering, University of Bradford, Bradford, BD7 1DP, United Kingdom*)

E-mail: s.s.ipson@bradford.ac.uk

References

1 AYACHE, N., and HANSEN, C.: 'Rectification of images for binocular and trinocular stereovision'. 9th Int. Conf. Pattern Recognition, 1988, IEEE, Rome, Italy, pp. 11–16
2 FUSIELLO, A., TRUCCO, E., and VERRI, A.: 'Rectification with unconstrained stereo geometry'. British Machine Vision Conf. BMVC97, (BMVA Press, Essex, UK, 1998), pp. 400–409
3 HARTLEY, R., and GUPTA, R.: 'Computing matched-epipolar projections'. Proc. IEEE Comput. Soc. Conf. Comput. Vision Pattern Recognit., (IEEE, 1993), pp. 549–555
4 ROBERT L., ZELLER C., FAUGERAS O., and HÉBERT, M.: 'Applications of nonmetric vision to some visually guided robotics' *in* ALOIMONOS, Y. (Ed.): 'Visual navigation' (Lawrence Erlbaum Associates, Mahwah, NJ, 1997), pp. 89–134
5 HARTLEY, R.I.: 'In defense of the eight-point algorithm', *IEEE Trans.*, 1997, **PAMI-19**, (6), pp. 580–593

Selection of image classifiers

G. Giacinto, F. Roli and G. Fumera

An approach to classifier combination based on the concept of 'dynamic classifier selection' is presented. The results reported show that the proposed approach enables effective image classification systems to be developed.

Introduction: In the field of pattern recognition, a number of image classification systems based on the combination of outputs of a set of different classifiers have been proposed [1]. For each pixel, the classification process is performed in parallel by different classifiers and the results are then combined. The combination methods proposed in the literature are based on 'voting' rules, statistical techniques, belief functions, and other 'classifier fusion' schemes [1]. As an example, the 'majority' voting rule interprets each classification result as a 'vote' for one of the data classes and assigns the input pattern to the class receiving the majority of votes. In such methods it is assumed that, for each pixel, different classifiers make different classification errors. In particular, Hansen and Salamon proved that the image classification accuracy obtained by combining different classifiers can be higher than that of the best individual classifier, only if the classifiers make 'independent' errors [2]. Unfortunately, in real image classification applications, it is usually difficult to design a set of classifiers satisfying such an assumption. On the other hand, it can be experimentally verified that it is easier to design a classifier ensemble where, for each pixel, at least one classifier can classify it correctly, while the remaining classifiers can also make the same error [3]. Accordingly, we and other researchers have recently independently proposed an alternative approach to classifier combination, based on the concept of 'dynamic classifier selection' (DCS) [3, 4]. DCS is based on the definition of a 'function' that, for each pixel, selects the classifier that is more likely to classify it correctly.

In this Letter we present two selection functions and a DCS algorithm based on them. Experimental results and comparisons are also reported.

Algorithm for dynamic classifier selection: Consider an image classification task for M data classes. Each class is assumed to represent a set of specific patterns, each pattern being an image pixel characterised by a feature vector $\mathbf{X}$. Also assume that K different classifiers, C_j, $j = 1, ..., K$, have been trained separately to solve the image classification task at hand. Our DCS algorithm is based on the concept of 'classifier's local accuracy' (CLA). The basic idea is to estimate the accuracy of each classifier in a local region of the feature space surrounding an unknown test pattern, and then to select the classifier with the highest value of this local